p-ISSN 1607-3274 Радіоелектроніка, інформатика, управління. 2025. № 4
e-ISSN 2313-688X Radio Electronics, Computer Science, Control. 2025. № 4

UDC 004.8

CLASSIFICATION OF HISTOLOGICAL IMAGES BASED ON CONVOLUTIONAL NEURAL NETWORKS

Liashchynskyi P. B. – Post-graduate student of the Department of Computer Engineering, West Ukrainian National University, Ternopil, Ukraine.

ABSTRACT

Context. Automated classification of histological images is of great importance for speeding up and improving the accuracy of diagnostics in medicine. Taking into account the complexity and high variability of histological structures, the use of deep learning and convolutional neural networks, in particular, is a promising direction in solving this problem.

The object of study is the process of classifying histological images using convolutional neural networks to determine and optimize the architecture with the highest accuracy rate.

Objective. The aim of this work is to develop an effective approach to histological image classification using convolutional neural networks that provides high accuracy through step-by-step optimization of the architecture and application of data expansion methods using affine transformations and synthesis based on diffusion models.

Method. The study includes four main stages. The first stage involves a comparative analysis of 12 well-known convolutional neural network architectures on a basic histological dataset. The second and third stages involve comparative analysis on extended data, including affine transformations and synthetic images generated by the diffusion model, respectively. The final, fourth stage involves a neuroevolutionary search for the optimal architectural cell. Once it is found, it is integrated into the model architecture, where for each layer a choice is made between certain blocks and the found cell. This approach allows to automatically form the optimal sequence of blocks in the model, which ensures the highest classification accuracy.

Results. The proposed approach improved the accuracy of histological image classification compared to the initial architectures. The addition of synthetic images to the training set provided an increase in model performance. The search for the optimal cell and its integration into the model with further optimization demonstrated an additional improvement in classification quality, increasing the accuracy to 94.9, 96.1, and 99.8% on each dataset, respectively.

Conclusions. The proposed approach allows achieving high accuracy of histological image classification through a step-by-step process that includes the use of classical convolutional neural network architectures, generation of synthetic data, and search for optimal architectural and hyperparametric configurations.

A software module for classifying histological images has been developed that can be used in an automatic diagnostic system.

KEYWORDS: convolutional neural networks, classification, optimization, histology.

ABBREVIATIONS

AI is an artificial intelligence;
CAD is a computer aided diagnosis;
CNN is a convolutional neural network;
CPU is a central processing unit;
CUDA is a compute unified device architecture;
DCNN is a deep convolutional neural network;
FTU is a functional tissue unit.
GB is a gigabyte;
GPU is a graphics processing unit;
LSTM is a long short-term memory;
NAS is a neural architecture search;
NNI is a neural network intelligence;
RAM is a random-access memory;
ROC is a receiver-operating characteristic;
UML is an unified modeling language;
VGG is a visual geometry group.

NOMENCLATURE

Acc is an accuracy metric;
B is a set of available blocks;
b_i is an available *i*-th block for neural network architecture;
C is a number of color channels;
Cell is a found optimized cell;
D is a dataset of histological images;
D is a number of nodes in the cell;
FN is a false negative, represents the number of FTU pixels being misclassified as background;
FN is a false positive, represents the number background pixels being misclassified as FTUs (due to misalignment);
H is a height of the image in pixels;
M is a model of neural network;
M^* is a model of neural network which showed the highest quality of classification;
M^+ is a developed and optimized model of neural network;
N is a number of images in the dataset;
n is a number of output classes;
O is a set of available operations;
p is a number of known CNN models;
R is a real numbers;
TN is a true negative, represents the number of background pixels that have been properly classified as background;
TP is a true positive, represents the number of FTU pixels that have been properly classified as FTU;
v is a number of layers in CNN;
W is a width of the image in pixels;
w_i is a width of the *i*-th block;
x_i is a *i*-th histology image;
Y is a set of all possible classes labels;
y_j is a *j*-th class label of histological image.

DOI 10.15588/1607-3274-2025-4-11

INTRODUCTION

Computer image recognition plays an important role in modern medicine. This process is key in diagnostics, including automated analysis of biomedical images.

Due to the rapid development of deep learning methods, it is now possible to process complex visual data contained in medical images of various types.

One of them is histological images, which are images of tissues obtained by microscopy after preliminary staining of samples.

These images are widely used in cancer diagnostics and help to assess the morphological structure of tissues and detect pathological changes [1–5]. However, the accuracy of the diagnosis in manual analysis largely depends on the experience of the specialist. This creates prerequisites for the implementation of automated solutions using neural networks.

Significant progress in the field of AI has led to the active implementation of CNNs in biomedical image analysis [6–12]. However, existing approaches often do not take into account the structural specificity of different tissue types, which reduces the accuracy of models in clinical settings. In addition, the impact of different convolutional neural network architectures on classification accuracy in the context of a limited number of annotated images is not sufficiently studied.

Thus, conducting experiments using well-known CNN architectures for histological image classification and further developing an optimized architecture to improve accuracy is a relevant and important task.

The object of study is the processes classification of histological images based on convolutional neural networks.

The subject of study are models, and tools for classifying histological images based on convolutional neural networks.

The purpose of the work is to improve the classification accuracy by optimizing the neural network architecture.

1 PROBLEM STATEMENT

Suppose we have a dataset of histological images consisting of N examples :

$$D = \{(x_i, y_j)\}_{i=1, j=1}^{N,3}.$$

Each image has a format: $x_i \in R^{H \times W \times C}$, with $y_j \in Y$ and $Y = \{1, 2, 3\}$.

We need to build a classification model that can be described as follows:

$$M : R^{H \times W \times C} \to Y.$$

That is, the model takes an image as an input and returns the label of the class to which this image belongs.

The problem of finding M^* can be solved by conducting experiments on a set of known CNN architectures:

$$\{M_1, M_2, ..., M_p\}.$$

The accuracy metric is described by the formula:

$$Acc = \frac{TP + TN}{TP + TN + FN + FP}.$$

The problem of finding an optimized version of M^+ can be solved in two steps: finding the optimal cell and building the macroarchitecture.

The process of finding a cell is to find the set of operations and the number of nodes that maximize the accuracy on the validation set:

$$Cell = \arg\max_d \, Acc(O, D).$$

Having found the optimal cell, we form the architecture at the macro level as a sequence of blocks. That is, the architecture is defined as an ordered sequence of $B = [b_1, b_2, \ldots, b_n]$.

The task is to find the optimal sequence of blocks and their number that maximizes the accuracy on the validation dataset:

$$M^+ = \arg\max_v \, Acc(Cell, D).$$

2 REVIEW OF THE LITERATURE

Image classification using convolutional neural networks is a fairly popular method. This technology has become especially popular in medical diagnostics.

Paper [13] describes the classification of benign and malignant subtypes of histopathological visualization of breast cancer using hybrid transfer learning based on CNN-LSTM.

The authors of [14] describe the analysis of histological images using hybrid methods for the early detection of multiclass breast cancer based on Fusion CNN and Handcrafted functions.

In [15], the authors propose a method to increase the robustness of CNNs to scanner and image variability (brightness, color, etc.) based on immunohistochemical images for epithelial segmentation in cervical histology.

The authors of [16] propose a new type of CNN based on a statistical filter. The paper describes the classification of histological tissue.

Paper [17] describes a distance regression and classification network for segmenting nuclei instances and classifying the type in histological images.

In [18], the authors propose a new classification method based on an extended decoding network based on the traditional U-shaped structure. The proposed method demonstrates good accuracy, reaching 0.92.

Paper [19] describes the use of CNNs for celiac disease classification. The authors also describe the use of

DOI 10.15588/1607-3274-2025-4-11

the same model for diagnosing carcinoma and Crohn's disease. The network showed good results in classifying 5 different diagnoses.

The authors of [20] conducted a detailed comparative analysis of different CNN models (VGG-16, AlexNet, ResNet-50) for classifying histological images to detect breast cancer. The BreakHis dataset was used for the test.

Paper [21] describes the use of CNNs with VGG19 architecture for the detection of oral squamous cell carcinoma.

The authors of [22] describe a trial model based on deep learning for four-class histological classification of colon tumors based on narrow band imaging.

Paper [23] describes colorectal cancer detection based on convolutional neural networks and a ranking algorithm.

The authors of [24] propose the FabNet CNN model for classifying histological images by accumulating layers closer to each other for further fusion of semantic and spatial features.

In [25], the authors used hybrid optimization using a deep convolutional neural network (DCNN) to identify and classify breast cancer types into different subclasses.

The authors of [26] describe the improvement of breast cancer grade classification using an integrated Swin Transformer.

Paper [27] describes CViTS-Net, a new CNN model for classifying histological images. The model achieves an accuracy of 96.06%.

Paper [28] describes the classification of histopathological images of lung cancer using transfer learning based on the EfficientNetB7 convolutional neural network model.

The authors of [29] improved the detection and classification of breast cancer by adjusting hyperparameters.

In [30], the authors describe the process of classifying histopathological images of breast cancer using CNNs and the VGG-19 model.

The authors of [31] propose a CNN architecture for classifying histopathological images of kidneys. The authors tested and compared the proposed architecture with seven state-of-the-art architectures.

Study [32] proposed a CNN-based classification of histopathological images of breast cancer. The authors used transfer learning to build four pre-trained models. Out of the four pre-trained models, DensNet201 achieved an accuracy of 91.37% and a sensitivity level of 100% at 200x magnification.

3 MATERIALS AND METHODS

A convolutional neural network is one of the most effective deep learning tools for image processing. Its architecture is designed to automatically detect characteristic features in input images using a cascade of specialized layers.

A CNN consists of input and output layers, and also has several hidden layers. CNNs usually consist of convolutional (responsible for detecting local patterns such as edges, textures, or more complex morphological features of tissues), subsampling (reduce the size of features while retaining the most important information, which helps to reduce computational complexity), normalization layers (stabilize the learning process and speed up model convergence), and fully connected layers (perform the final interpretation of features and classification based on the generalized information from the previous layers).

The general architecture of a convolutional neural network is shown in Fig. 1. The illustration shows the sequential passage of an image through the layers of the model – from the initial filtering to the final class prediction.

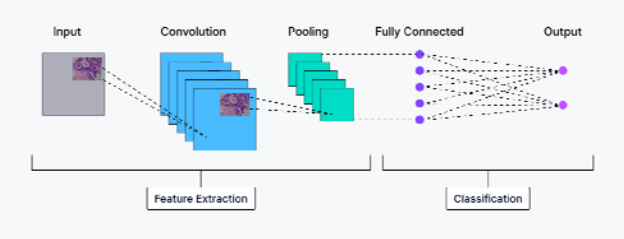

Figure 1 – General CNN architecture

Fig. 2 shows the general process of automatic image classification using neural networks.

This diagram shows the full cycle of an artificial intelligence system for the task of classifying histological images, illustrating the effectiveness of CNNs in medical computer vision tasks.

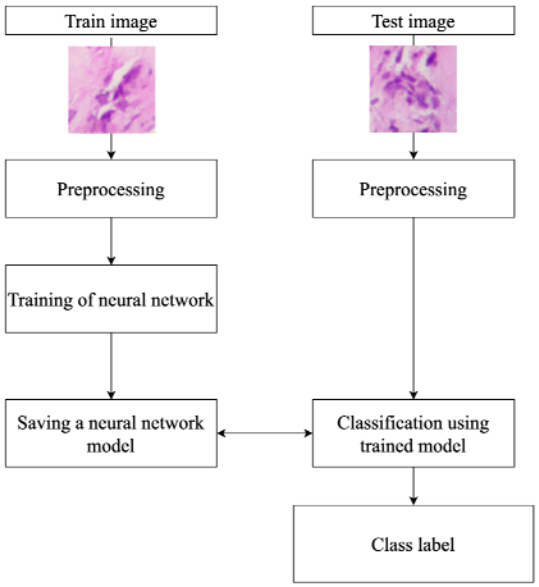

Figure 2 – General scheme of the image classification process using neural networks

As you can see from Fig. 2, the train image needs to be pre-processed (noise reduction or brightness equalization, resizing, etc.). The neural network is trained on images, and then its model is saved. As a result of

DOI 10.15588/1607-3274-2025-4-11

training, the model is able to classify images. To do this, we submit the Test Image as an input, pre-process it, and apply the already trained model for classification, after which we get the result – the label of the class to which the image belongs.

This process needs to be repeated several times until we go through all the following architectures that have been selected for the experiments: AlexNet, VGG-16, ResNet 18, Wide ResNet, ResNeXt, GoogLeNet, Inception V3, EfficientNet, EfficientNetV2, MobileNet V2, MobileNet V3, ConvNeXt.

The general scheme of the study and the process of finding an optimized architecture is shown in Fig. 3.

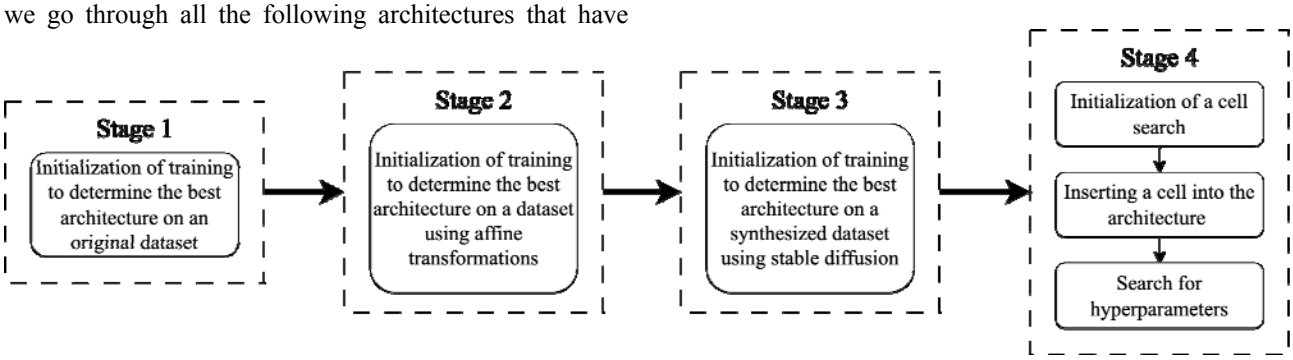

Figure 3 – General scheme of the process of research and search for an optimized architecture

As shown in Fig. 3, the experimental methodology is divided into several sequential stages (Stage 1–4), each of which performs an important function in the research process.

Stage 1 involves initial testing of various neural network architectures on the original histological image dataset.

The purpose of this stage is to preliminarily evaluate the performance of the models without additional transformations of the input data. This allows you to determine the baseline level of accuracy against which the results of the following stages can be compared.

In Stage 2 and Stage 3, similar experiments are performed, but on extended versions of the dataset. At these stages, affine transformations are applied to the images:

– affine distortions (scaling, rotation, mirroring), that increase the variability of the sample and allow the model to better generalize information;

– diffusion models – modern generative methods used to synthesize additional samples to expand the data.

Stage 4 focuses on architecture search and optimization. First, Neural Architecture Search is performed to find the optimal structure of the computing cell (for this purpose, the method developed and proposed by the authors in [33] was used), which is then integrated into the overall model as a building block. After that, the hyperparametric optimization of the updated architecture is performed, which allows to achieve maximum classification accuracy by adjusting the parameters.

To find the optimal network architecture, we used the regularized evolution algorithm, which is a variant of the evolutionary algorithm used to find the best neural network architecture in the model space. This method, which was presented in [34], has the following features:

1) population – a fixed number of architectures are stored;

2) parent selection – the best architecture is selected from a random subset of the population based on performance;

3) mutation – a random change is applied to the selected architecture (e.g., changing the layer, number of filters, etc.);

4) replacement – a new architecture is added to the population, and the oldest architecture is removed (this step is called “regularization” because it limits the accumulation of old solutions).

Evolutionary search with regularization is an effective NAS method that balances between using the best architectures and exploring new options. The pseudocode of the algorithm is shown in Fig. 4.

```
archive ← ∅                    // Stores all evaluated architectures
queue ← empty FIFO structure   // Current population of models

// Initial random population generation
while |queue| < MAX_POPULATION do
    individual.arch ← CREATE_RANDOM_ARCH()
    individual.score ← TRAIN_AND_ASSESS(individual.arch)
    add individual to end of queue
    add individual to archive
end while

// Evolutionary search loop
while |archive| < MAX_EVALUATIONS do
    pool ← ∅                   // Candidates for parent selection

    // Sample parent candidates randomly
    while |pool| < POOL_SIZE do
        candidate ← random element from queue
        add candidate to pool
    end while

    // Select best-performing parent
    parent ← element in pool with highest score

    // Generate and evaluate a mutated child
    offspring.arch ← MUTATE_ARCHITECTURE(parent.arch)
    offspring.score ← TRAIN_AND_ASSESS(offspring.arch)

    // Add offspring to population and archive
    add offspring to end of queue
    add offspring to archive

    // Remove oldest individual from population
    remove first element from queue
end while

// Return the best discovered architecture
return element in archive with highest score
```

Figure 4 – Pseudocode of the regularized evolution algorithm

DOI 10.15588/1607-3274-2025-4-11

To search for the optimal cell, several available operations are predefined (Fig. 5), which are randomly selected in a certain sequence until the highest accuracy is achieved.

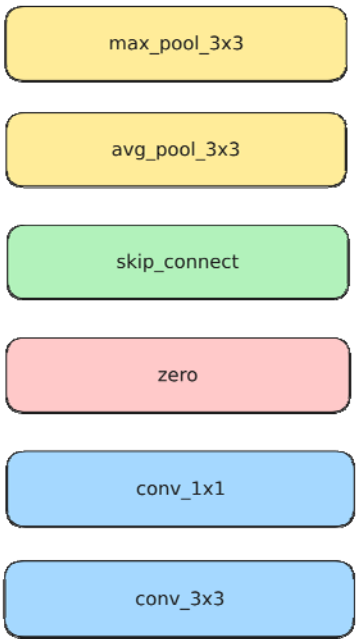

Figure 5 – Available operations pool

Let us consider each of them in more detail [35].

1) Pool. The pooling layer is used to reduce the dimensionality of the input data. At this stage, feature maps are reduced after convolution layers. Popular types of pooling are: average, maximum, and global. Only two types of pooling are used in the cell operations: average with a 3×3 kernel and maximum with a 3×3 kernel.

2) Skip connect. The input data is not transformed after the operation is applied. This operation can be considered as a function that accepts data and immediately returns it. This operation allows the output of a node to be directly linked to the input of another node. This operation helps to avoid gradient damping. This operation is also called the identity function.

3) Zero. The zero operation replaces the output of a node with a matrix of zeros. This operation can be used to remove a node from the cell architecture and effectively simplify the architecture. Applying this operation between two nodes means that there is no connection between them.

4) Conv. The input data is multiplied with the convolution kernel and then the result is summed. The output is a new matrix. This operation reflects the standard convolution function in neural networks.

The cell architecture is encoded according to the example shown in Fig. 6.

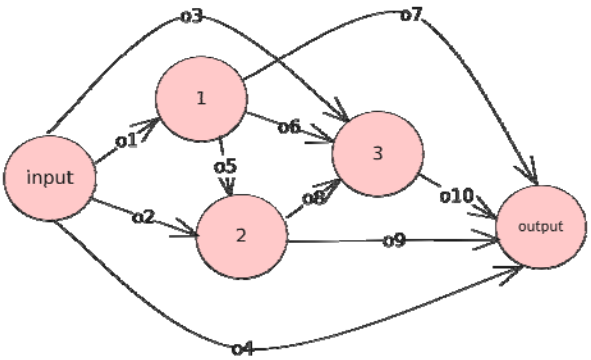

Figure 6 – An example of coding cell architecture

The letter X represents a digit from 0 to 5, i.e. o = {0, 1, 2, 3, 4, 5}. These digits correspond to the indices of the elements in the set of available operations (see Fig. 4). The first three digits in the code represent operations that connect the input node with nodes 1, 2, 3, and output, respectively (o1, o2, o3, o4). The next three digits encode the operations between nodes 1, 2, 3 (o5, o6) and output (o7). The next two digits encode the operations between nodes 2, 3, and output (o8, o9). The last digit encodes the operation between node 3 and output (o10).

To find the optimal network architecture, the choice is made from among the available blocks, including the optimal cell found.

The evolutionary algorithm searches for the sequence with the highest accuracy.

4 EXPERIMENTS

The experimental studies were implemented using the Python 3 programming language, which is a standard in the field of machine learning and scientific computing. PyTorch was chosen as the main library for building, training, and testing neural networks, as it is one of the most popular open source frameworks that provides flexibility in model design and a user-friendly interface for working with GPUs.

All experiments were performed in the Google Colab cloud environment, which allows you to use computing resources directly from your browser. To ensure high performance, we used an NVIDIA A100 GPU with 40 GB of memory and 83.5 GB of RAM, which allowed us to effectively train large neural networks and search for optimal architectures.

To implement the automatic search for neural network architectures, we used the NNI framework, which provides powerful tools for the experimental study of neural architectures, including support for popular NAS methods.

The software implementation is divided into two main modules: search.py and optimize.py.

The search.py script is responsible for automatically searching through the space of possible architectures, generating them, and initially evaluating them according to a given metric. It also implements the logic for

DOI 10.15588/1607-3274-2025-4-11

interacting with the search strategy and saving the results of each experiment.

The optimize.py script is used in the last step – optimizing the best architecture found. At this stage, the hyperparameters are fine-tuned, the model is retrained, and the final evaluation of its quality is performed.

The structure of the modules and the logic of building experiments is implemented using object-oriented programming. Fig. 7 shows a class diagram that illustrates the key components of the search.py module and their interrelationships.

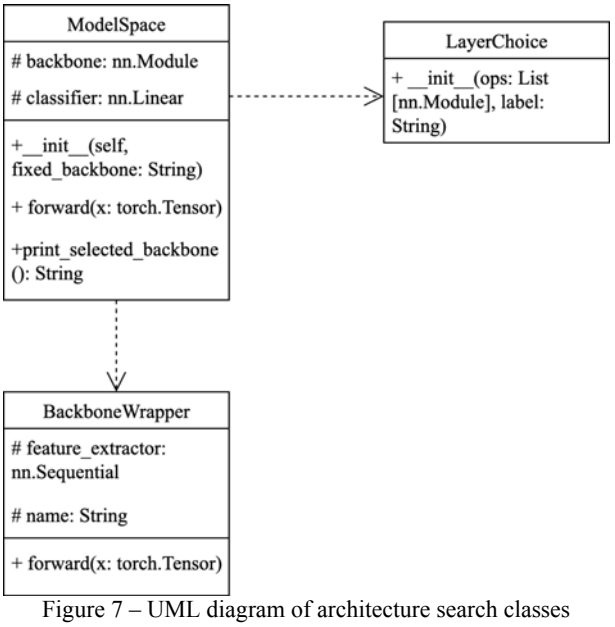

Figure 7 – UML diagram of architecture search classes

The BackboneWrapper class serves as a wrapper for each architecture to unify the interface. It is used to describe models from the PyTorch library.

The ModelSpace class describes the implementation of the model selected by LayerChoice. In addition, through the fixed_backbone parameter, it can be passed an architecture from predefined ones. This is useful when you need to test a specific model.

After performing the search and obtaining the architecture with the highest accuracy rate, we can use the same script to conduct experiments on a sample of data with affine distortion and a synthesized sample of histological images.

The dataset used in the study consists of histological images with three categories of labels: G1, G2, and G3, which correspond to different degrees of tissue differentiation. Each image has a resolution of 4096×3286 pixels, which provides high detail for analysis.

Fig. 8 illustrates examples of histological images for each of the classes, which allows you to visually assess the difference between them and emphasizes the importance of applying powerful deep learning methods for their effective classification.

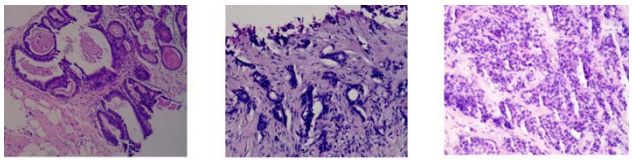

Figure 8 – Example of histological images for each class

To conduct the experiments, all images were previously resized to a uniform size of 512×512 pixels. This reduction in resolution allowed us to strike a balance between preserving enough morphological detail for analysis and reducing the computational load on the model during training.

To improve the generalizability of the model, a number of affine distortions were applied. The images were processed using the Torchvision library, which is part of the PyTorch stack. During these distortions, random horizontal or vertical mirroring, random rotation by 90 or 180 degrees, random crop with scaling, rotation without edge artifacts, and image shift without edge artifacts were applied to the images.

Each image underwent the described transformations to create two augmented copies, which were stored in the corresponding directory along with the original. Thus, for each image, a total of three variants are created (1 original and 2 fragmented).

To conduct computer experiments and generate images, we used the Stable Diffusion Web UI from Jarvis Labs with an A6000 Ampere GPU (CUDA 12.3) with 48 GB of video memory, 32 GB of RAM, and 7 CPUs.

This configuration ensures high performance for AI-generated images, allowing to effectively use the capabilities of the Stable Diffusion model to generate high-quality results.

The model v1-5-pruned-emaonly.safetensors was used for training and generation.

The diffusion models were trained for 33 epochs with the number of steps being 10000. The total training time was 45 minutes. One step took 0.27 seconds and one epoch took 81 seconds.

Images were generated on 5 prints saved at steps 2000, 4000, 6000, 8000, and 10000. Each print generated 1000 images, for a total of 5000 images.

The generation time was 2 hours 37 minutes and 41 seconds for G1, 2 hours 19 minutes and 58 seconds for G2, and 2 hours 38 minutes and 12 seconds for G3.

Fig. 9 shows examples of synthesized images generated by the diffusion models.

In the Stage 1, Stage 2, and Stage 3, each model was trained for 25 epochs, and the number of possible architectures was 12. The batch size for each architecture was the same, with 64 images.

For the Stage 4, the number of optimization cycles was 20, the population size was 30, and the number of epochs was 25.

DOI 10.15588/1607-3274-2025-4-11

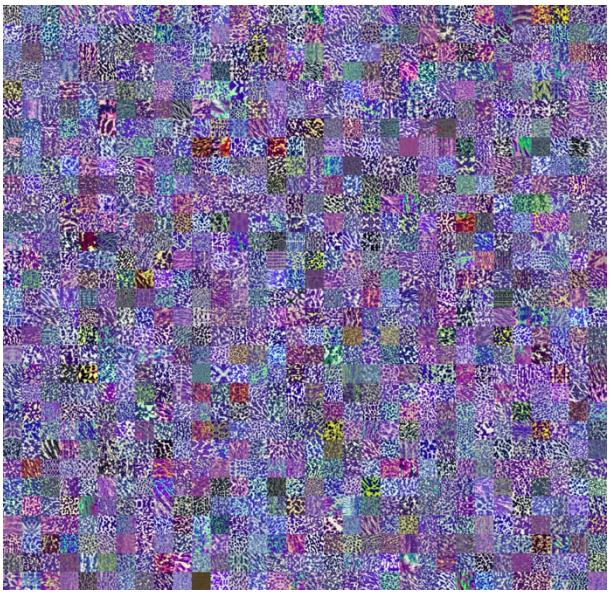

Figure 9 – Example of synthesized histological images

As a result, the architectures with the highest accuracy coefficient were identified, which made it possible to assess the impact of data preparation on model accuracy, find the optimal cell, and optimize the neural network model to improve classification accuracy.

5 RESULTS

As a result of the experiments conducted in the first stage (Stage 1), the results of which are shown in Table 1, the RegNet architecture demonstrated the highest efficiency. All the results presented are sorted in descending order of the main accuracy metric, which allows us to clearly identify the best architectures among the models considered.

Table 1 – Results of experiments on an original dataset

№	Name	*Acc*, %
1	RegNet	90,7
2	Inception V3	90,2
3	MobileNet V2	90
4	Wideresnet	88,3
5	ResNeXt	87,7
6	EfficientNet	84,3
7	VGG16	84.2
8	ResNet	84
9	GoogLeNet	82
10	AlexNet	81,9
11	ConvNeXt	80
12	MobileNet V3	36,7

The further experiments conducted in the second (Stage 2) and third (Stage 3) stages are detailed in Table 2–3, respectively. Similarly to the first stage, the results are also sorted in descending order for easy analysis and comparison.

Table 2 – Results of experiments on a dataset using affine transformations

№	Name	*Acc*, %
1	RegNet	91,1
2	Wideresnet	90,9
3	ResNeXt	90,84
4	MobileNet V2	90,8
5	Inception V3	90, 7
6	EfficientNet	89,6
7	ResNet	89,1
8	GoogLeNet	87,3
9	AlexNet	86
10	ConvNeXt	84
11	VGG16	82,9
12	MobileNet V3	34,4

Table 3 – Results of experiments on a synthesized dataset

№	Name	*Acc*, %
1	RegNet	96,6
2	ResNeXt	94,3
3	Wideresnet	94
4	Inception V3	93, 1
5	MobileNet V2	92,9
6	EfficientNet	92,5
7	ResNet	92,1
8	GoogLeNet	92
9	AlexNet	91,9
10	ConvNeXt	88,5
11	VGG16	86,5
12	MobileNet V3	38,4

Analyzing the results presented in Table 1–3, we can confidently state that the RegNet architecture consistently demonstrated the highest classification accuracy on each of the studied datasets. Accordingly, RegNet was chosen as the base model for further work on optimizing and improving the architecture.

The general structure of RegNet is shown in Fig. 10, and its detailed structure is shown in Table 4.

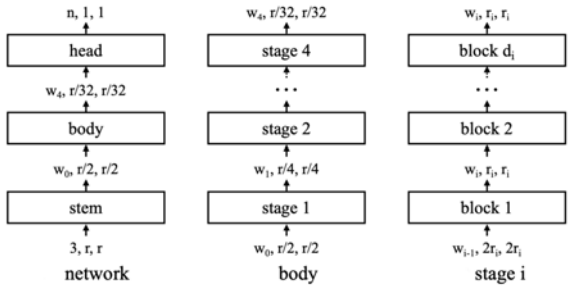

Figure 10 – General RegNet structure

Each network consists of a stem (stride-two 3×3 conv with $w_0 = 32$ output channels), followed by the network body that performs the bulk of the computation, and then a head (average pooling followed by a fully connected layer) that predicts n output classes.

The network body is composed of a sequence of stages that operate at progressively reduced resolution. Each stage consists of a sequence of identical blocks, except the first block which uses stride-two conv. While the general structure is simple, the total number of possible network configurations is vast [36].

DOI 10.15588/1607-3274-2025-4-11

Table 4 – Detailed RegNet structure

Layer name	Layer type	Params	Output shape
Stem	Stride-two 3×3 conv	Kernel = 3, stride = 2	32×112×112
Stage 1	Sequence of X Blocks	Stride = 2 (for the first block)	24×56×56
Stage 2	Sequence of X Blocks	Stride = 2 (for the first block)	56×28×28
Stage 3	Sequence of X Blocks	Stride = 2 (for the first block)	152×14×14
Stage 4	Sequence of X Blocks	Stride = 2 (for the first block)	368×7×7
Head	AvgPool + Fully Connected Layer		3
Block structure			

Table 5 shows the comparative results of classification accuracy obtained for the original RegNet architecture and optimized version developed in this study. The results are presented for different types of datasets, which allows us to assess the versatility and adaptability of the optimized model. In particular, the optimized architecture demonstrates an improvement in classification accuracy, which indicates the success of the applied improvement methods. This underscores the effectiveness of the chosen optimization approach, which allows us to improve the model's performance without significantly increasing its complexity.

Table 5 – Comparison between the original version of RegNet and the developed version

Name	Dataset	*Acc*, %
RegNet	Original	90,7
Developed		94,9
RegNet	Affines	91,1
Developed		96,1
RegNet	Synthesized	95,6
Developed		99,8

The architecture of the CustomCell shown in Fig. 11 consists of six nodes that are interconnected by a complex network of edges. Each edge corresponds to a specific operation that transforms the input features and is selected from a set of basic operations, including avg_pool_3x3, skip_connect, zero, conv_1x1, conv_3x3, max_pool_3x3 in a different sequence.

The structure of the cell is organized in such a way that each node aggregates information from several previous nodes using selected operations, which provides flexibility and multi-level feature integration. Thanks to this topology, the cell can balance between preserving the original information through pass-through paths and its gradual transformation through convolution and pooling.

As a result, the resulting cell has an individual composition of operations and connections that is maximally adapted to solve a specific task of classifying histological images.

The cell architecture is coded as follows: 23141–3232–334–21–2.

The architecture of the developed neural network is shown in Fig. 12 and consists of 6 layers.

The structure of the developed neural network is shown in Table 6.

The neural network has a simple and efficient structure with an initial convolutional layer, a series of optimized cells (CustomCell), convolutional and pooling operations, and a final classifier. The network has 16 channels across the entire depth, with dimensionality reduction occurring only once (Layer 2). The main computing unit is an optimized CustomCell.

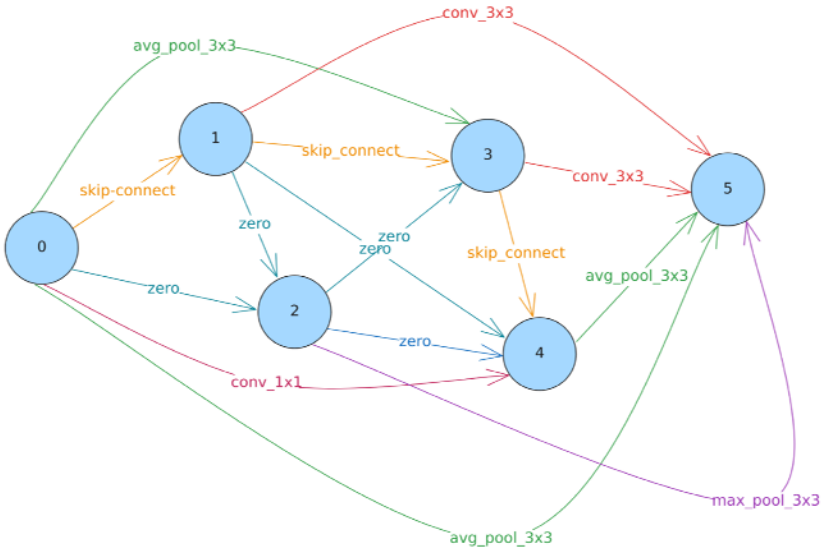

Figure 11 – Found cell architecture

DOI 10.15588/1607-3274-2025-4-11

The ROC curve of the optimized architecture is shown in Fig. 13. The result shows the classification accuracy on the dataset synthesized by diffusion models. The accuracy reached 99.8%.

6 DISCUSSION

As a result of the study, a new optimized architecture for histological image classification was developed, which demonstrates improved performance compared to known architectures. To quantify the performance of the models, we used the Accuracy metric, which is the key metric in classification tasks.

Tables 1–3 illustrate the results of comparisons among various known architectures, allowing to analyze their performance on test datasets.

In turn, Table 5 presents the results of the experiments conducted in the fourth stage (Stage 4), where the accuracy of the classical RegNet architecture and the developed optimized model on different types of histological datasets is compared.

In contrast to the traditional RegNet architecture, the optimized model, the details of which are shown in Fig. 12 and Table 6, is characterized by much greater flexibility. This flexibility is manifested in the ability to dynamically select types of operations, adjust the network depth, and vary its topology. This approach allows us to adapt the model to the specifics of a particular dataset, which in turn leads to an increase in classification accuracy on each of the datasets under consideration.

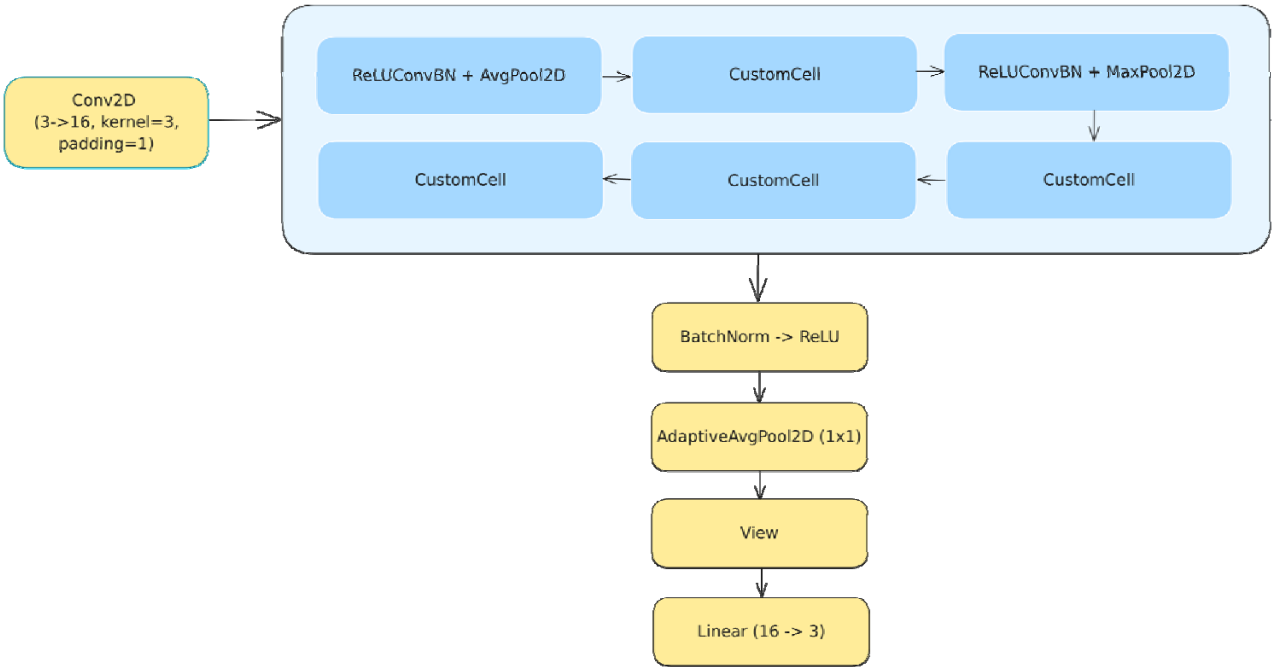

Figure 12 – Developed CNN architecture

Table 6 – Developed CNN structure

Layer name	Layer type	Params	Output shape
Stem	Conv2D	Kernel = 3, stride = 1, padding = 1	16×512×512
Layer 0	ReLUConvBN + AvgPool2D	Kernel = 3, stride = 1, padding = 1	16×512×512
Layer 1	CustomCell	Kernel = 3, stride = 1, padding = 1, Nodes = 6	16×512×512
Layer 2	ReLUConvBN + MaxPool2D	Kernel = 3, stride = 2, padding = 1	16×256×256
Layer 3	CustomCell	Kernel = 3, stride = 1, padding = 1, Nodes = 6	16×256×256
Layer 4	CustomCell	Kernel = 3, stride = 1, padding = 1, Nodes = 6	16×256×256
Layer 5	CustomCell	Kernel = 3, stride = 1, padding = 1, Nodes = 6	16×256×256
Last act	BatchNorm + ReLU		16×256×256
Global pooling	AdaptiveAvgPool2D		16×1×1
Flatten	View		16
Classifier	Linear		3

DOI 10.15588/1607-3274-2025-4-11

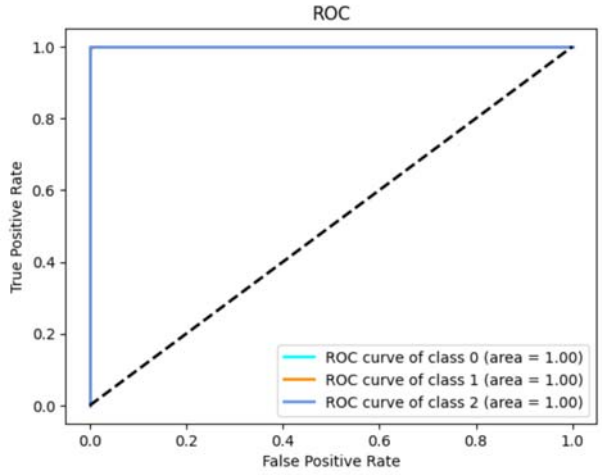

Figure 13 – ROC-curve of a developed architecture

In addition, the optimized architecture has lower memory requirements because it is more compact than the original RegNet. It is important to note that this model stores spatial information in intermediate layers more efficiently, which is critical for histological image classification tasks where cell and tissue structure patterns are highly significant.

In this study, the experiments were not conducted with high-resolution images due to limited hardware resources and a considerable training time.

The maximum image size used was 512×512 pixels. To work with higher resolutions, it is necessary to increase the amount of available GPU memory, which is a promising area for future research.

It should also be noted that the experimental base was limited to histological images of breast cancer. Accordingly, one of the key areas of further work is to expand the scope of the model by adapting it to the classification of histological images of other organs and working with higher resolution data. This opens up additional opportunities for implementing the developed architecture in clinical practice and research.

CONCLUSIONS

The paper solves the scientific and applied problem of improving the accuracy of histological image classification by gradually optimizing the architecture of a convolutional neural network and improving the learning process by using synthetic and transformed data.

For the first time, a consistent approach to building a classification model has been implemented, which includes:

1) training and comparison of 12 known CNN architectures on different types of histological datasets to determine the model with the highest accuracy, which allowed us to assess the impact of different data preparation options on classification results;

2) integrating the cell found by the method described in [35] into the CNN model and further optimizing it to improve accuracy.

The scientific novelty is to improve the approach to building efficient CNN architectures for histological image classification:

– for the first time, the effectiveness of using synthetic histological images generated by the diffusion model for training a classifier was investigated;

– the process of step-by-step comparison, training, and optimization has been improved, which has led to a significant increase in accuracy.

The practical significance is the software implementation of a module that can be integrated into an automatic diagnostic system to improve the quality of medical research [37].

Prospects for further research is the development of a CAD system. The system uses neural networks to segment, classify, and generate biomedical images [38, 39].

ACKNOWLEDGEMENTS

The authors of the article express their gratitude to the Department of Pathological Anatomy with a Sectional Course and Forensic Medicine of I. Ya. Horbachevsky Ternopil National Medical University (Ternopil, Ukraine) for providing histopathological images of breast cancer and personally to Doctor of Medical Sciences, Professor, and Head of the Department Petro Romanovych Selskyy.

REFERENCES

1. Underwood J. C. E. More than meets the eye: the changing face of histopathology, *Histopathology,* 2016, Vol. 70, № 1, pp. 4–9. DOI: 10.1111/his.13047.
2. Schafer et al. K. A. Use of Severity Grades to Characterize Histopathologic Changes, Toxicologic Pathology, 2018, Vol. 46, № 3, pp. 256–265. DOI: 10.1177/0192623318761348.
3. Ho C., Rodig S. J. Immunohistochemical markers in lymphoid malignancies: Protein correlates of molecular alterations, *Seminars in Diagnostic Pathology,* 2015, Vol. 32, № 5, pp. 381–391. DOI: 10.1053/j.semdp.2015.02.016.
4. Li Z. et al. Large-scale retrieval for medical image analytics: A comprehensive review, *Medical Image Analysis,* 2018, Vol. 43, pp. 66–84. DOI: 10.1016/j.media.2017.09.007.
5. Zeiser FE. et al. Breast cancer intelligent analysis of histopathological data: A systematic review, *Applied Soft Computing,* 2021, Vol. 113, P. 107886. DOI: 10.1016/j.asoc.2021.107886.
6. Houssein E. H. et al. Deep and machine learning techniques for medical imaging-based breast cancer: A comprehensive review, *Expert Systems with Applications,* 2020, Vol. 167, P. 114161. DOI: 10.1016/j.eswa.2020.114161.
7. He W. et al. A review: The detection of cancer cells in histopathology based on machine vision, *Computers in Biology and Medicine*, 2022, Vol. 146, P. 105636. DOI: 10.1016/j.compbiomed.2022.105636.
8. Komura D., Ochi M., Ishikawa S. Machine learning methods for histopathological image analysis: Updates in 2024, *Computational and Structural Biotechnology Journal.* – 2024, Vol. 27, pp. 383–400. DOI: 10.1016/j.csbj.2024.12.033.
9. Abdelsamea M. M. et al. A survey on artificial intelligence in histopathology image analysis, *WIREs Data Mining and Knowledge Discovery*, 2022, Vol. 12, № 6, P. e1474. DOI: 10.1002/widm.1474.

DOI 10.15588/1607-3274-2025-4-11

10. Yan T. et al. Convolutional Neural Network with Parallel Convolution Scale Attention Module and ResCBAM for Breast Histology Image Classification, *Heliyon*, 2024, Vol. 10, № 10, P. e30889. DOI: 10.1016/j.heliyon.2024.e30889.
11. Rafiq A. et al. Detection and Classification of Histopathological Breast Images Using a Fusion of CNN Frameworks, *Diagnostics*, 2023, Vol. 13, № 10, P. 1700. DOI: 10.3390/diagnostics13101700.
12. Peng C. C., Lee B. R.Enhancing colorectal cancer histological image classification using transfer learning and ResNet50 CNN Model, *2023 IEEE 5th Eurasia Conference on Biomedical Engineering, Healthcare and Sustainability (ECBIOS) : proceedings*, 2023, pp. 36–40. DOI: 10.1109/ECBIOS57802.2023.10218590.
13. Srikantamurthy M. M. et al. Classification of benign and malignant subtypes of breast cancer histopathology imaging using hybrid CNN-LSTM based transfer learning, *BMC Medical Imaging*, 2023, Vol. 23, № 1. DOI: 10.1186/s12880-023-00964-0.
14. Al-Jabbar M. et al. Analyzing Histological Images Using Hybrid Techniques for Early Detection of Multi-Class Breast Cancer Based on Fusion Features of CNN and Handcrafted, *Diagnostics*, 2023, Vol. 13, № 10, P. 1753. DOI: 10.3390/diagnostics13101753.
15. Ruiz FM. et al. CNN stability training improves robustness to scanner and IHC-based image variability for epithelium segmentation in cervical histology, *Frontiers in Medicine*, 2023, Vol. 10. DOI: 10.3389/fmed.2023.1173616.
16. Ünlükal N. et al. Histological tissue classification with a novel statistical filter□based convolutional neural network, *Anatomia, Histologia, Embryologia,* 2024, Vol. 53, № 4. DOI: 10.1111/ahe.13073.
17. Dogar G. M., Shahzad M., Fraz M. M. Attention augmented distance regression and classification network for nuclei instance segmentation and type classification in histology images, *Biomedical Signal Processing and Control,* 2023, Vol. 79, P. 104199. DOI: 10.1016/j.bspc.2022.104199.
18. Xiao S. et al. A scale and region-enhanced decoding network for nuclei classification in histology image, *Biomedical Signal Processing and Control,* 2023, Vol. 83, P. 104626. DOI: 10.1016/j.bspc.2023.104626.
19. Carreras J. Celiac Disease Deep Learning Image Classification Using Convolutional Neural Networks / J. Carreras // Journal of Imaging. – 2024. – Vol. 10, № 8. – P. 200. – DOI: 10.3390/jimaging10080200.
20. Chandana Mani R. K., Kamalakannan J. The Comparative Study of CNN models for Breast Histopathological Image Classification, *2023 International Conference on Computer Communication and Informatics (ICCCI), Coimbatore, India, 23–25 January 2023 : proceedings*, 2023. DOI: 10.1109/iccci56745.2023.10128352.
21. Weber A. et al. AI-Based Detection of Oral Squamous Cell Carcinoma with Raman Histology, *Cancers,* 2024, Vol. 16, № 4, P. 689. DOI: 10.3390/cancers16040689.
22. Shimizu T. et al. A trial deep learning-based model for four-class histologic classification of colonic tumor from narrow band imaging, *Scientific Reports,* 2023, Vol. 13, № 1. DOI: 10.1038/s41598-023-34750-3.
23. Karthikeyan A., Jothilakshmi S., Suthir S. Colorectal cancer detection based on convolutional neural networks (CNN) and ranking algorithm, *Measurement: Sensors*, 2024, Vol. 31, P. 100976. DOI: 10.1016/j.measen.2023.100976.
24. Amin M. S., Ahn H. FabNet: A Features Agglomeration-Based Convolutional Neural Network for Multiscale Breast Cancer Histopathology Images Classification, *Cancers*, 2023, Vol. 15, № 4, P. 1013. DOI: 10.3390/cancers15041013.
25. Sawant D., Kundale J., Varma P. Hybrid Deep Learning based Multi-Classification of Breast Cancer Approach using Histology Images, *2024 2nd International Conference on Advancement in Computation & Computer Technologies (InCACCT), Gharuan, India, 2–3 May 2024 : proceedings,* 2024. DOI: 10.1109/incacct61598.2024.10551068.
26. Sreelekshmi V., Pavithran K., Jyothisha J. Nair SwinCNN: An Integrated Swin Trasformer and CNN for Improved Breast Cancer Grade Classification, *IEEE Access,* 2024, Vol. 12, P. 1. DOI: 10.1109/access.2024.3397667.
27. Kanadath A., Jothi J. A. A., Urolagin S. CViTS-Net: A CNN-ViT Network with Skip Connections for Histopathology Image Classification, *IEEE Access,* 2024, Vol. 12, P. 1. DOI: 10.1109/access.2024.3448302.
28. Muniasamy A. et al. Lung cancer histopathology image classification using transfer learning with convolution neural network model, *Technology and Health Care,* 2023, Vol. 32, № 2, pp. 1–12. DOI: 10.3233/thc-231029.
29. Kousalya K., Saranya T. Improved the detection and classification of breast cancer using hyper parameter tuning, *Materials Today: Proceedings,* 2021, Vol. 81. DOI: 10.1016/j.matpr.2021.03.707.
30. Kanimozhi S., Priyadarsini S. Breast Cancer Histopathological Image Classification Using CNN and VGG-19, *2024 Third International Conference on Intelligent Techniques in Control, Optimization and Signal Processing (INCOS), Krishnankoil, Virudhunagar distric.* Tamil Nadu, India, 14–16 March 2024 : proceedings, 2024. DOI: 10.1109/incos59338.2024.10527543.
31. Chanchal A. K. et al. Classification and grade prediction of kidney cancer histological images using deep learning [Electronic resource], *Multimedia Tools and Applications,* 2024, Vol. 83, pp. 78247–78267. DOI: 10.1007/s11042-024-18639-5.
32. Simonyan E. O., Badejo J. A., Weijin J. S. Histopathological breast cancer classification using CNN, *Materials Today: Proceedings,* 2023, Vol. 105, pp. 268–275. DOI: 10.1016/j.matpr.2023.10.154.
33. Berezsky O. et al. Synthesis of Convolutional Neural Network architectures for biomedical image classification, *Biomedical Signal Processing and Control,* 2024, Vol. 95, P. 106325. DOI: 10.1016/j.bspc.2024.106325.
34. Real E. et al. Regularized evolution for image classifier architecture search, *Proceedings of the AAAI Conference on Artificial Intelligence : proceedings*, 2019, pp. 4780–4789. DOI: 10.48550/arXiv.1802.01548.
35. Berezsky O. M., Liashchynskyi P. B. Method of generative-adversarial networks searching architectures for biomedical images synthesis, *Radio Electronics, Computer Science, Control,* 2024, № 1, P. 104. DOI: 10.15588/1607-3274-2024-1-10.
36. Radosavovic I. et al. Designing Network Design Spaces, *2020 IEEE/CVF Conference on Computer Vision and Pattern Recognition (CVPR) : proceedings*, 2020. DOI: 10.48550/arXiv.2003.13678.
37. Berezsky O. M., Liashchynskyi P. B. Development of the architecture of a computer aided diagnosis system in medicine, *Applied Aspects of Information Technology*, 2024, Vol. 7, № 4, P. 359–369. DOI: 10.15276/aait.07.2024.25.
38. Berezsky O. M., Pitsun O. Y. Evaluation methods of image segmentation quality, *Radio Electronics, Computer Science,*

DOI 10.15588/1607-3274-2025-4-11

Control, 2018, № 1, pp. 119–128. DOI: 10.15588/1607-3274-2018-1-14.

39. [Berezsky O. M., Liashchynskyi P. B. et al. Deep network-based method and software for small sample biomedical image generation and classification, *Radio Electronics, Computer Science, Control*, 2024, № 4, P. 76. DOI: 10.15588/1607-3274-2023-4-8.

Received 13.07.2025.
Accepted 14.10.2025.

УДК 004.8

КЛАСИФІКАЦІЯ ГІСТОЛОГІЧНИХ ЗОБРАЖЕНЬ НА ОСНОВІ ЗГОРТКОВИХ НЕЙРОННИХ МЕРЕЖ

Лящинський П. Б. – аспірант кафедри комп'ютерної інженерії, Західноукраїнський національний університет, Тернопіль, Україна.

АНОТАЦІЯ

Актуальність. Велике значення для прискорення та підвищення точності діагностики в медицині має автоматизована класифікація гістологічних зображень. Беручи до уваги складність і високу варіативність гістологічних структур, застосування глибокого навчання і згорткових нейронних мереж зокрема, є перспективним напрямком у вирішенні цієї задачі.

Об'єктом дослідження є процес класифікації гістологічних зображень з допомогою згорткових нейронних мереж для визначення та оптимізації архітектури із найвищим показником точності.

Мета роботи. Метою роботи є розробка ефективного підходу до класифікації гістологічних зображень із використанням згорткових нейронних мереж, який забезпечує високу точність за рахунок поетапної оптимізації архітектури та застосування методів розширення даних з допомогою афінних перетворень та синтезу на основі дифузійних моделей.

Метод. Дослідження включає чотири основні етапи. На першому проведено порівняльний аналіз 12 відомих архітектур згорткових нейронних мереж на базовому гістологічному датасеті. Другий та третій етапи передбачають порівняльний аналіз на розширених даних, що включають афінні перетворення та синтетичні зображення, згенеровані дифузійною моделлю відповідно. На фінальному, четвертому етапі виконується нейроеволюційний пошук оптимальної архітектурної комірки. Після її знаходження вона інтегрується у розроблену архітектуру моделі, де для кожного шару здійснюється вибір між певними блоками та знайденою коміркою. Такий підхід дозволяє автоматично сформувати оптимальну послідовність блоків у моделі, що забезпечує найвищу точність класифікації.

Результати. Запропонований підхід дозволив покращити точність класифікації гістологічних зображень порівняно з початковими архітектурами. Додавання синтетичних зображень до навчального набору забезпечило приріст продуктивності моделей. Пошук оптимальної комірки та її інтеграція в модель з подальшою оптимізацією продемонстрував додаткове покращення якості класифікації, збільшивши точність до 94,9, 96,1 та 99,8% на кожному датасеті відповідно.

Висновки. Запропонований підхід дозволяє досягнути високої точності класифікації гістологічних зображень завдяки поетапному процесу, що включає використання класичних архітектур згорткових нейронних мереж, генерацію синтетичних даних та пошук оптимальних архітектурних і гіперпараметричних конфігурацій. Розроблено програмний модуль класифікації гістологічних зображень, який може бути використаний у системі автоматичного діагностування.

КЛЮЧОВІ СЛОВА: згорткові нейронні мережі, класифікація, оптимізація, гістологія.

ЛІТЕРАТУРА

1. Underwood J. C. E. More than meets the eye: the changing face of histopathology / J. C. E. Underwood // Histopathology. – 2016. – Vol. 70, № 1. – P. 4–9. DOI: 10.1111/his.13047.
2. Use of Severity Grades to Characterize Histopathologic Changes / [K. A. Schafer et al.] // Toxicologic Pathology. – 2018. – Vol. 46, № 3. – P. 256–265. DOI: 10.1177/0192623318761348.
3. Ho C. Immunohistochemical markers in lymphoid malignancies: Protein correlates of molecular alterations / C. Ho, S. J. Rodig // Seminars in Diagnostic Pathology. – 2015. – Vol. 32, № 5. – P. 381–391. DOI: 10.1053/j.semdp.2015.02.016.
4. Large-scale retrieval for medical image analytics: A comprehensive review / [Z. Li et al.] // Medical Image Analysis. – 2018. – Vol. 43. – P. 66–84. DOI: 10.1016/j.media.2017.09.007.
5. Breast cancer intelligent analysis of histopathological data: A systematic review / [FE. Zeiser et al.] // Applied Soft Computing. – 2021. – Vol. 113. – P. 107886. DOI: 10.1016/j.asoc.2021.107886.
6. Deep and machine learning techniques for medical imaging-based breast cancer: A comprehensive review / [E. H. Houssein et al.] // Expert Systems with Applications. – 2020. – Vol. 167. – P. 114161. DOI: 10.1016/j.eswa.2020.114161.
7. A review: The detection of cancer cells in histopathology based on machine vision / [W. He et al.] // Computers in Biology and Medicine. – 2022. – Vol. 146. – P. 105636. DOI: 10.1016/j.compbiomed.2022.105636.
8. Komura D. Machine learning methods for histopathological image analysis: Updates in 2024 / D. Komura, M. Ochi, S. Ishikawa // Computational and Structural Biotechnology Journal. – 2024. – Vol. 27. – P. 383–400. DOI: 10.1016/j.csbj.2024.12.033.
9. A survey on artificial intelligence in histopathology image analysis / [M. M. Abdelsamea et al.] // WIREs Data Mining and Knowledge Discovery. – 2022. – Vol. 12, № 6. – P. e1474. DOI: 10.1002/widm.1474.
10. Convolutional Neural Network with Parallel Convolution Scale Attention Module and ResCBAM for Breast Histology Image Classification / [T. Yan et al.] // Heliyon. – 2024. – Vol. 10, № 10. – P. e30889. DOI: 10.1016/j.heliyon.2024.e30889.
11. Detection and Classification of Histopathological Breast Images Using a Fusion of CNN Frameworks / [A. Rafiq et al.] // Diagnostics. – 2023. – Vol. 13, № 10. – P. 1700. DOI: 10.3390/diagnostics13101700.
12. Peng C. C. Enhancing colorectal cancer histological image classification using transfer learning and ResNet50 CNN Model / C. C. Peng, B. R. Lee // 2023 IEEE 5th Eurasia Conference on Biomedical Engineering, Healthcare and Sustainability (ECBIOS) : proceedings. – 2023. – P. 36–40. DOI: 10.1109/ECBIOS57802.2023.10218590.

DOI 10.15588/1607-3274-2025-4-11

13. Classification of benign and malignant subtypes of breast cancer histopathology imaging using hybrid CNN-LSTM based transfer learning / [M. M. Srikantamurthy et al.] // BMC Medical Imaging. – 2023. – Vol. 23, № 1. DOI: 10.1186/s12880-023-00964-0.
14. Analyzing Histological Images Using Hybrid Techniques for Early Detection of Multi-Class Breast Cancer Based on Fusion Features of CNN and Handcrafted / [M. Al-Jabbar et al.] // Diagnostics. – 2023. – Vol. 13, № 10. – P. 1753. DOI: 10.3390/diagnostics13101753.
15. CNN stability training improves robustness to scanner and IHC-based image variability for epithelium segmentation in cervical histology / [FM. Ruiz et al.] // Frontiers in Medicine. – 2023. – Vol. 10. DOI: 10.3389/fmed.2023.1173616.
16. Histological tissue classification with a novel statistical filter□based convolutional neural network / [N. Ünlükal et al.] // Anatomia, Histologia, Embryologia. – 2024. – Vol. 53, № 4. DOI: 10.1111/ahe.13073.
17. Dogar G. M. Attention augmented distance regression and classification network for nuclei instance segmentation and type classification in histology images / G. M. Dogar, M. Shahzad, M. M. Fraz // Biomedical Signal Processing and Control. – 2023. – Vol. 79. – P. 104199. DOI: 10.1016/j.bspc.2022.104199.
18. A scale and region-enhanced decoding network for nuclei classification in histology image / [S. Xiao et al.] // Biomedical Signal Processing and Control. – 2023. – Vol. 83. – P. 104626. DOI: 10.1016/j.bspc.2023.104626.
19. Carreras J. Celiac Disease Deep Learning Image Classification Using Convolutional Neural Networks / J. Carreras // Journal of Imaging. – 2024. – Vol. 10, № 8. – P. 200. – DOI: 10.3390/jimaging10080200.
20. Chandana Mani R. K. The Comparative Study of CNN models for Breast Histopathological Image Classification / R. K. Chandana Mani, J. Kamalakannan // 2023 International Conference on Computer Communication and Informatics (ICCCI), Coimbatore, India, 23–25 January 2023 : proceedings. – 2023. DOI: 10.1109/iccci56745.2023.10128352.
21. AI-Based Detection of Oral Squamous Cell Carcinoma with Raman Histology / [A. Weber et al.] // Cancers. – 2024. – Vol. 16, № 4. – P. 689. DOI: 10.3390/cancers16040689.
22. A trial deep learning-based model for four-class histologic classification of colonic tumor from narrow band imaging / [T. Shimizu et al.] // Scientific Reports. – 2023. – Vol. 13, № 1. DOI: 10.1038/s41598-023-34750-3.
23. Karthikeyan A. Colorectal cancer detection based on convolutional neural networks (CNN) and ranking algorithm / A. Karthikeyan, S. Jothilakshmi, S. Suthir // Measurement: Sensors. – 2024. – Vol. 31. – P. 100976. DOI: 10.1016/j.measen.2023.100976.
24. Amin M. S. FabNet: A Features Agglomeration-Based Convolutional Neural Network for Multiscale Breast Cancer Histopathology Images Classification / M. S. Amin, H. Ahn // Cancers. – 2023. – Vol. 15, № 4. – P. 1013. DOI: 10.3390/cancers15041013.
25. Sawant D. Hybrid Deep Learning based Multi-Classification of Breast Cancer Approach using Histology Images / D. Sawant, J. Kundale, P. Varma // 2024 2nd International Conference on Advancement in Computation & Computer Technologies (InCACCT), Gharuan, India, 2–3 May 2024 : proceedings. – 2024. DOI: 10.1109/incacct61598.2024.10551068.
26. Sreelekshmi V. SwinCNN: An Integrated Swin Trasformer and CNN for Improved Breast Cancer Grade Classification / V. Sreelekshmi, K. Pavithran, Jyothisha J. Nair // IEEE Access. – 2024. – Vol. 12. – P. 1. DOI: 10.1109/access.2024.3397667.
27. Kanadath A. CViTS-Net: A CNN-ViT Network with Skip Connections for Histopathology Image Classification / A. Kanadath, J. A. A. Jothi, S. Urolagin // IEEE Access. – 2024. – Vol. 12. – P. 1. DOI: 10.1109/access.2024.3448302.
28. Lung cancer histopathology image classification using transfer learning with convolution neural network model / [A. Muniasamy et al.] // Technology and Health Care. – 2023. – Vol. 32, № 2. – P. 1–12. DOI: 10.3233/thc-231029.
29. Kousalya K. Improved the detection and classification of breast cancer using hyper parameter tuning / K. Kousalya, T. Saranya // Materials Today: Proceedings. – 2021. – Vol. 81. DOI: 10.1016/j.matpr.2021.03.707.
30. Kanimozhi S. Breast Cancer Histopathological Image Classification Using CNN and VGG-19 / S. Kanimozhi, S. Priyadarsini // 2024 Third International Conference on Intelligent Techniques in Control, Optimization and Signal Processing (INCOS), Krishnankoil, Virudhunagar district, Tamil Nadu, India, 14–16 March 2024 : proceedings. – 2024. DOI: 10.1109/incos59338.2024.10527543.
31. Classification and grade prediction of kidney cancer histological images using deep learning [Electronic resource] / [A. K. Chanchal et al.] // Multimedia Tools and Applications. – 2024. – Vol. 83. – P. 78247–78267. DOI: 10.1007/s11042-024-18639-5.
32. Simonyan E. O. Histopathological breast cancer classification using CNN / E. O. Simonyan, J. A. Badejo, J. S. Weijin // Materials Today: Proceedings. – 2023. – Vol. 105. – P. 268–275. DOI: 10.1016/j.matpr.2023.10.154.
33. Synthesis of Convolutional Neural Network architectures for biomedical image classification / [O. Berezsky et al.] // Biomedical Signal Processing and Control. – 2024. – Vol. 95. – P. 106325. – DOI: 10.1016/j.bspc.2024.106325.
34. Regularized evolution for image classifier architecture search / [E. Real et al.] // Proceedings of the AAAI Conference on Artificial Intelligence : proceedings. – 2019. – P. 4780–4789. DOI: 10.48550/arXiv.1802.01548.
35. Berezsky O. M. Method of generative-adversarial networks searching architectures for biomedical images synthesis / O. M. Berezsky, P. B. Liashchynskyi // Radio Electronics, Computer Science, Control. – 2024. – № 1. – P. 104. DOI: 10.15588/1607-3274-2024-1-10.
36. Designing Network Design Spaces / [I. Radosavovic et al.] // 2020 IEEE/CVF Conference on Computer Vision and Pattern Recognition (CVPR) : proceedings. – 2020. DOI: 10.48550/arXiv.2003.13678.
37. Berezsky O. M. Development of the architecture of a computer aided diagnosis system in medicine / O. M. Berezsky, P. B. Liashchynskyi // Applied Aspects of Information Technology. – 2024. – Vol. 7, № 4. – P. 359–369. DOI: 10.15276/aait.07.2024.25.
38. Berezsky O. M. Evaluation methods of image segmentation quality / O. M. Berezsky, O. Y. Pitsun // Radio Electronics, Computer Science, Control. – 2018. – № 1. – P. 119–128. DOI: 10.15588/1607-3274-2018-1-14.
39. Deep network-based method and software for small sample biomedical image generation and classification / [O. M. Berezsky, P. B. Liashchynskyi et al.] // Radio Electronics, Computer Science, Control. – 2024. – № 4. – P. 76. DOI: 10.15588/1607-3274-2023-4-8.

DOI 10.15588/1607-3274-2025-4-11